HASL-25

health and safety laboratory

EXTERNAL ENVIRONMENTAL RADIATION MEASUREMENTS IN THE UNITED STATES

L. R. SOLON, W. M. LOWDER, A. V. ZILA, H. D. LEVINE, H. BLATZ, M. EISENBUD

MARCH 11, 1958

UNITED STATES ATOMIC ENERGY COMMISSION
NEW YORK OPERATIONS OFFICE

HASL-25

EXTERNAL ENVIRONMENTAL RADIATION MEASUREMENTS IN THE UNITED STATES

L. R. Solon
W. M. Lowder
A. V. Zila
H. D. LeVine
H. Blatz
M. Eisenbud

U. S. ATOMIC ENERGY COMMISSION
NEW YORK OPERATIONS OFFICE
HEALTH AND SAFETY LABORATORY

ABSTRACT

During the Summer of 1957 ion chamber measurements were made of the external environmental radiation in locations throughout the United States. The purpose of these measurements was to establish the approximate range of population exposures to the penetrating radiation component, cosmic radiation and terrestrial gamma radiation, but excluding terrestrial beta radiation.

The natural levels encountered ranged from a low of 8.4 microroentgens/hour along the Pennsylvania Turnpike to a high of 38.6 microroentgens/hour at the summit of Pikes Peak. Among the major United States cities visited, Denver, Colorado exhibited the highest radiation levels with a range of 16.6 to 22.4 microroentgens/hour. Elevated levels associated with fallout from nuclear weapons tests, were encountered in eastern Arkansas and the Black Hills of South Dakota.

The results of this survey are compared with the estimates of other investigators; including, the measurements of Hess, Neher, Compton, and the calculations of Burch and Libby.

EXTERNAL ENVIRONMENTAL RADIATION MEASUREMENTS IN THE UNITED STATES

L. R. Solon*
W. M. Lowder
A. V. Zila
H. D. LeVine
H. Blatz
M. Eisenbud

Recent interest in the dose to man from natural radioactivity has been stimulated by the assumption by many geneticists of a linear relationship between radiation dose and the incidence of genetic mutations. Although this has not been demonstrated at the low dose rates prevailing in nature, the likelihood of such a relationship has led to the suggestion that geographical variations in the frequency of spontaneous mutations may be correlated ultimately with differences in the radiation dose to populations.[1] This question has recently been reviewed by Gopal-Ayengar.[2]

The studies of the dose received by man from naturally occurring ionizing radiations can be divided into that received from external and internal sources. The dose to the germplasm is primarily due to the external radiation, although one internal source, potassium-40, does deliver a dose to the reproductive organs amounting to about fifteen milliroentgens/year.[3,4]

Studies of the radiation dose from external natural sources have been reviewed by Sievert,[3] Libby,[4] and Lowder,[5] and extensive sets of measurements with particular emphasis on dwellings have been reported by Hultqvist[6] in Sweden. Although measurements have been made in this country by Hess[7] and Neher,[8] no systematic study of the environmental radiation dose rate over an extensive area of the United States has been reported previously.

During the Summer of 1957 this Laboratory made measurements in the United States to establish the approximate range of population exposures to cosmic and terrestrial gamma radiation. An effort was made to obtain results which would be representative of the unperturbed natural background, affected as little as possible by the occasional substantial variations in the observed natural radiation levels produced by localized sources (e.g., proximity of granite buildings, brick paving, fallout, etc.).

Measurements were made with a 20-liter, air-filled, polyethylene-walled ionization chamber at atmospheric pressure. The chamber was kept inside an automobile under essentially identical field conditions of loading and ionization chamber orientation. It had been established previously that the attenuation by the vehicle did not affect the measured values in an important way (about five percent). The ionization current was measured

---

* United States Atomic Energy Commission, Health and Safety Laboratory, New York.

with a vibrating reed electrometer, connected as a continuously reading voltmeter, driving a pen recorder. To shield completely against beta radiation, the chamber was mounted in an aluminum container so that, including the polyethylene wall, the gas volume was enclosed by 1.08 g/cm^2 of material, corresponding to the Feather range of a 2.26 Mev beta particle.

As is well known, minute alpha contamination in an ion chamber at atmospheric pressure can produce an ion current which may be of the same order as the ion current being measured. For this reason it is important that the effect of the contamination be measured or that the alpha-produced current be suppressed. Several different methods have been used by previous investigators. In our measurements we have resorted to a technique which relies on the difference in electric fields necessary to effect total collection of ion pairs produced by particles of low and high specific ionization; i.e., electrons from gamma or cosmic-ray interactions and alpha particles, respectively. The details of the instrumentation and technique are described in Appendix II.

Readings were taken at one hundred fifty-four locations in nineteen states, between New York and Utah. The natural environmental radiation levels encountered ranged from a low of 8.4 microroentgens/hour along the Pennsylvania Turnpike to a high of 38.6 microroentgens/hour at the summit of Pikes Peak (Alt. 14,110 ft.). A summary of the dose rates measured in the principal cities along the route is given in Table I and a complete tabulation of all measurements in Appendix I. A map of the itinerary is shown at the beginning of Appendix I.

Of the major cities listed, Denver had the highest natural background with an average of 18.5 $\pm$ 1.5 microroentgens/hour, a level almost twice that found in eastern and midwestern cities.

These measurements were made during part of the period of Operation Plumbob, the 1957 series of United States continental weapons tests at the National Test Station in Nevada, and these tests influenced certain of the measured values. Elevated levels were encountered in eastern Arkansas (26.0 - 50.2 microroentgens/hour) and in the Black Hills of South Dakota (22.0 - 33.8 microroentgens/hour). That the initial elevated levels at these two locations were attributable to fresh fallout was demonstrated by the reduction in the measured levels by 50 - 75 percent upon resurvey about three weeks later. A resurvey of the Denver area almost three months later furnished results essentially identical with the earlier survey.

In general, one finds that the background radiation level increases as a function of decreasing barometric pressure. This is shown in Fig. 1, for which the data have been reduced in the following way. Where the radiation levels were demonstrably elevated from local sources, they were removed from consideration. The remaining one hundred thirty measurements were classified according to the barometric pressure at the time of measurement in intervals of one inch of mercury. The average values and standard

deviations of the measured background and pressure for each pressure interval were then calculated and these results are exhibited in Fig. 1. The number of observations for each pressure interval is indicated in parentheses. The four Pikes Peak observations are plotted separately as "P", though they have also been included in the averages. The point with barometric pressure, 21.2 inches Hg, has a large standard deviation in the measured radiation level, being derived from only two observations which differed substantially (Pikes Peak Highway, 35.0 microroentgens/hour and Leadville, Colorado, 23.5 microroentgens/hour).

On the same figure are plotted the adapted ionization chamber measurements of the intensity of the cosmic radiation alone as reported by Bowen, Millikan, and Neher[9] and by Compton.[10] The most important difference between these two sets of cosmic-ray data is the amount of filtration of the ion chambers used, the first being thin-walled measurements (0.5 mm of steel), while Compton's measurements were made with the argon gas cavity shielded with 5 cm of lead and 2.5 cm of bronze in addition to the steel wall of the chamber.

It should be pointed out that even at sea level the numerical value of the total cosmic-ray intensity is not something on which there is universal agreement. Burch, in his critical review,[11] concludes that the best value for the ionization intensity at sea level may be deduced from the experimental work of Clay. This value is 1.77 ion pairs/cm^3-sec (3.1 microroentgens/hour) compared to Neher's value[12] of 2.74 ion pairs/cm^3-sec (4.8 microroentgens/hour). Hess' value[7] of 1.96 ion pairs/cm^3-sec (3.4 microroentgens/hour) falls between these two. It would appear that the discrepancies are too large to depend merely on differences in ionization chamber wall thickness or calibration technique.

Comparing the results of our measurements with the cosmic-ray data of Bowen, Millikan, and Neher, it is clear that a substantial part of the variability in mean outdoor radiation intensities over extensive areas in the United States is attributable to the variation in the cosmic radiation intensity with altitude. Most of the measurements made at higher altitudes were obtained in Colorado, and the shift of the total radiation curve in Fig. 1 away from the cosmic-ray curve at higher altitudes may be due to a higher terrestrial radiation component in the mountainous areas of Colorado.

Expressed on an annual basis, our measurements indicate a range of approximately 70 to 175 millirads/year for external environmental radiation dose rates in populated areas in the United States, with the lower dose rates prevailing in the more populated eastern and midwestern states. This compares with estimates made in the recent report of the National Academy of Sciences on the biological effects of atomic radiation,[13] which gives an average annual background dose of about 135 millirads and a maximum dose of about 170 millirads in populated areas.

Location	Range of Radiation Levels (microroentgens/hr)	Mean Annual Dose (millirads)*	Average Pressure (inches Hg)	Atypical Radiation Levels (microroentgens/hr)
Harrisburg, Pa.	9.6 - 11.9 (2)	88	29.8	-
Pittsburgh, Pa.	9.8 - 13.9 (3)	96	29.2	-
Cleveland, Ohio	10.5 - 11.8 (2)	91	29.4	
Toledo, Ohio	8.7 - 10.0 (2)	76	29.5	14.9 (over granite paving stone)
Chicago, Ill.	10.3 - 11.6 (4)	88	29.4	17.0 (adjacent to U.S. Post Office Bldg. of granite construction)
Madison, Wisc.	10.1 - 10.4 (3)	84	29.1	-
Minneapolis-St. Paul, Minn.	9.1 - 12.5 (4)	92	29.3	-
Sioux Falls, S. Dakota	11.5 - 11.8 (2)	95	28.8	-
Cheyenne, Wyo.	17.2 - 17.6 (2)	142	24.4	-
Denver, Colo.	16.6 - 19.4 (10)	147	25.0	22.4 (between U.S. Mint and City and County Bldgs.)
Colorado Springs, Colo.	19.3 - 22.3 (4)	168	24.2	-
Grand Junction, Colo.	15.7 - 18.4 (3)	138	25.5	-
Albuquerque, N. Mexico	13.8 - 14.5 (4)	116	25.2	-
Amarillo, Texas	12.9 - 13.6 (4)	108	26.4	-
Oklahoma City, Okla.	9.9 - 10.5 (4)	84	28.7	-
Tulsa, Okla.	10.8 - 11.6 (4)	92	29.3	-
Little Rock, Ark.	12.8 - 13.3 (2)	106	29.7	-
Memphis, Tenn.	9.4 - 11.0 (2)	83	29.8	13.3 (near brick apartment house)
Chattanooga, Tenn.	11.1 - 12.3 (2)	95	29.6	14.8 (near brick-faced motel units)
				16.1 (on narrow business street; 8th between Broad and Market)

* Dose in soft tissue, assuming constant dose rate.
1 rad = 100 ergs/gm, 1 microroentgen/hr = 8.152 mrad/yr.

Table I. Environmental radiation levels measured in principal United States cities during August, 1957. The number of observations for each range are shown in parentheses. Elevated radiation levels produced by localized sources are shown in the last column.

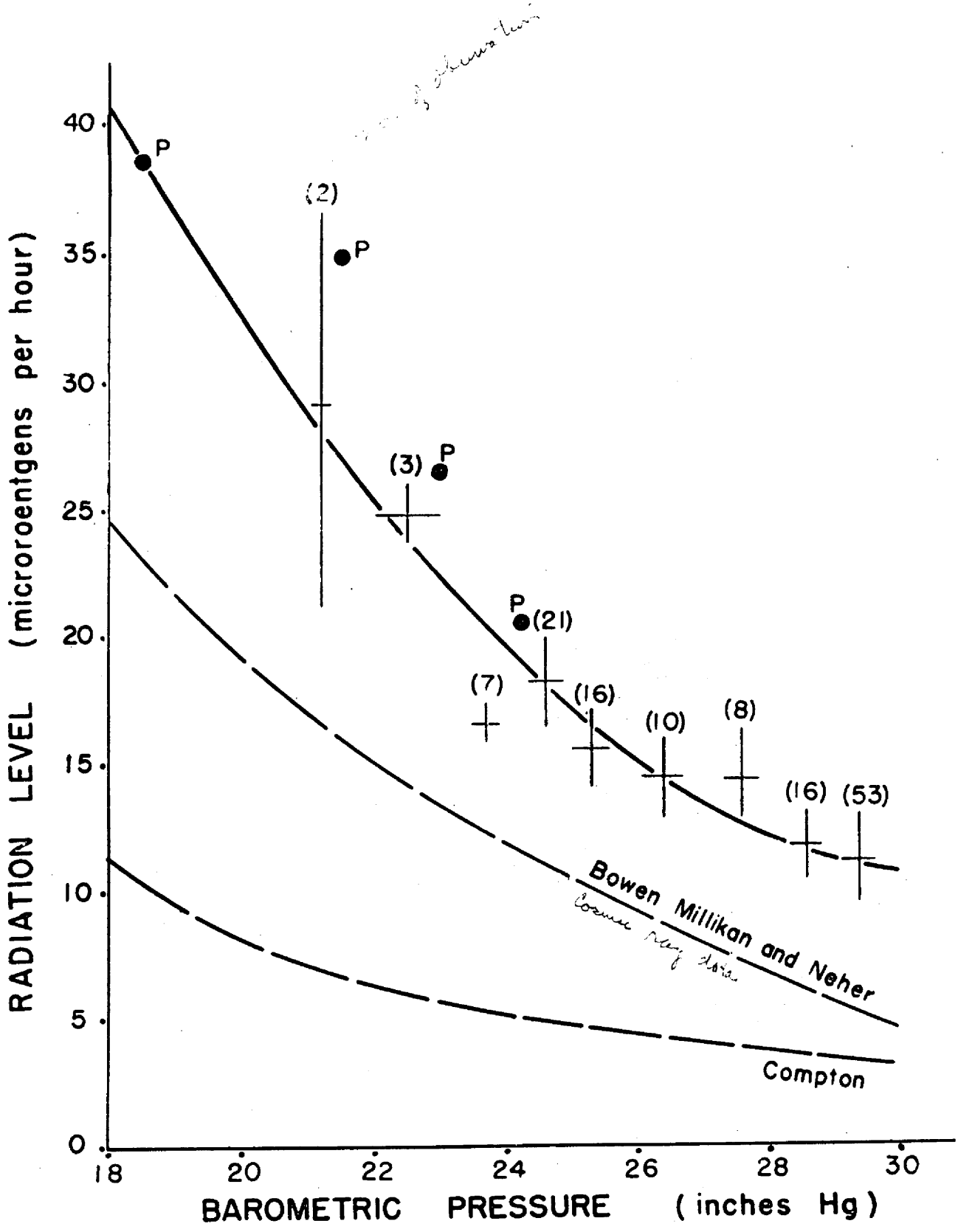

Figure 1. Variation of environmental radiation dose rates with barometric pressure. The lower curves are for cosmic radiation intensities alone. The number of observations incorporated in each point are shown in parentheses. Points marked "P" are observations on Pikes Peak.

REFERENCES

1. Carter, T. C., Proc. International Conf. on Peaceful Uses of Atomic Energy, Geneva, 1955, 11, 384 (1956).

2. Gopal-Ayengar, A. R., in Effect of Radiation on Human Heredity, World Health Organization, Geneva (1957).

3. Sievert, R. M., in Effect of Radiation on Human Heredity, World Health Organization, Geneva (1957).

4. Libby, W. F., Science, 122, 57 (1955).

5. Lowder, W. M. and Solon, L. R., NYO-4712 (1956).

6. Hultqvist, B., Kgl. Svenska Vetenskapsakad. Handl. (4) 6, No. 3 (1956)

7. Hess, V. F. and O'Donnell, G. A., J. Geophys. Research, 56, 4 (1951).

8. Neher, H. V., Science, 125, 3257 (1957).

9. Bowen, I. S., Millikan, R. A., and Neher, H. V., Phys. Rev., 53, 111 (1938).

10. Compton, A. H., Phys. Rev. 43, 387 (1933).

11. Burch, P. R. J., Proc. Phys. Soc. A 57, 421 (1954).

12. Neher, H. V., in Progress in Cosmic Ray Physics, Vol. 1, North-Holland, Amsterdam (1952).

13. The Biological Effects of Atomic Radiation, Summary Report of the Committee on Genetic Effects to the National Academy of Sciences, Nat. Acad. of Sciences - Nat. Research Council, Washington, D. C. (1956).

APPENDIX I

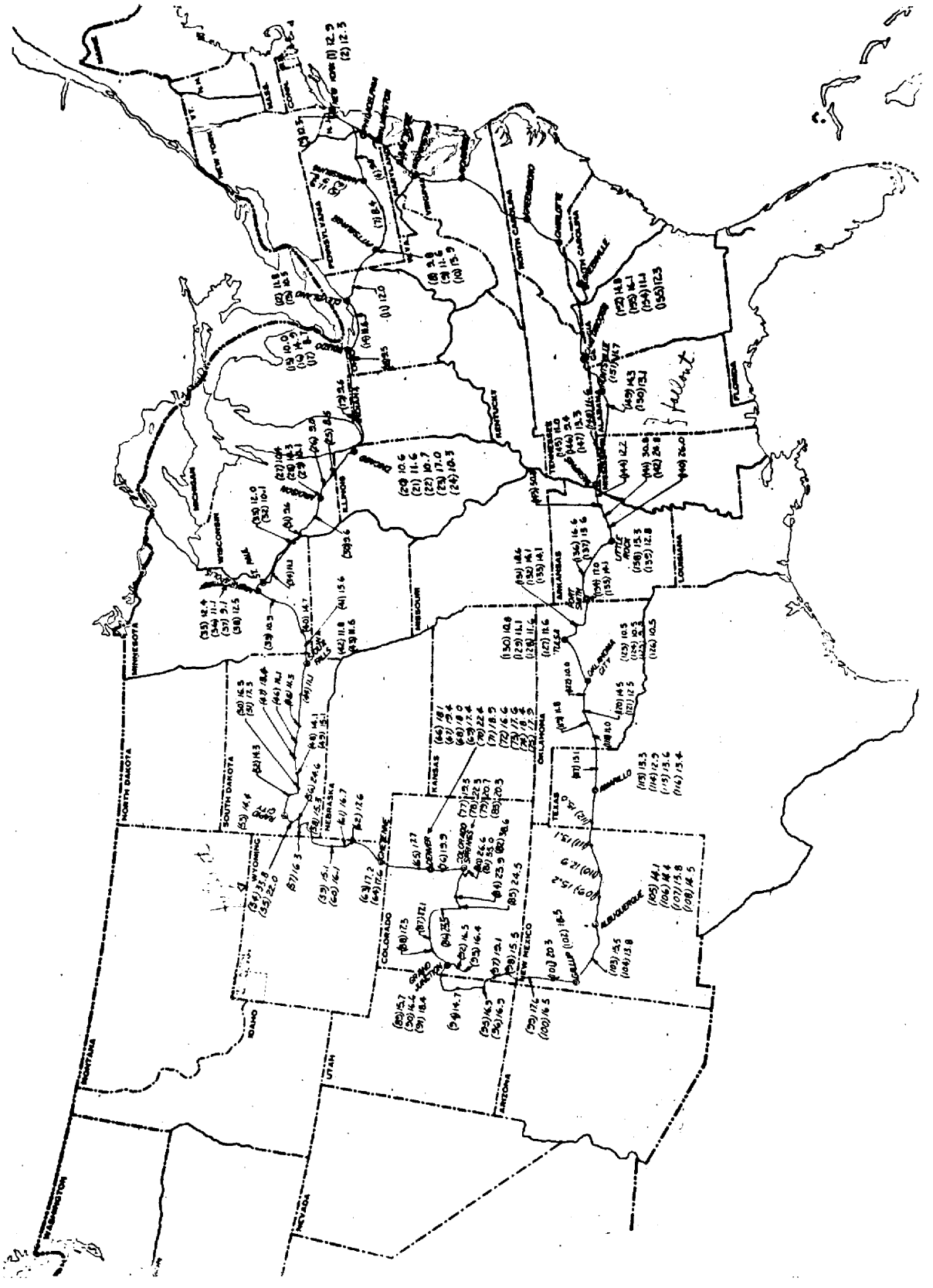

Itinerary of Survey - August, 1957

	LOCATION	RADIATION LEVEL (μr/hr)	DATE AND TIME (1957)	PRESSURE (Inches)	TEMPERATURE (°C)	COMMENTS
1.	Pelham, N. Y.	12.9	Aug. 11, 1:15 P.M. (EDT)	29.93	33.5	33 Young Avenue, North Pelham - Asphalt Street
2.	New York City, N.Y.	12.3	Aug. 12, 8:30 A.M.	29.89	26.8	3963 Orloff Ave., Borough of Bronx - Driveway adjacent to brick house
3.	Newark, New Jersey	10.3	Aug. 12, 9:30 A.M.	30.04	26.0	First Service Area, New Jersey Turnpike
4.	Denver, Pennsylvania	9.0	Aug. 12, 12:30 P.M.	29.57	30.3	Service Area, Pennsylvania Turnpike
5.	Harrisburg, Pennsylvania	11.9	Aug. 12, 2:10 P.M.	29.71	34.5	South Second and Washington near downtown area
6.	Harrisburg, Pennsylvania	9.6	Aug. 12, 2:45 P.M.	29.71	33.0	Second and Market - downtown area
7.	Pennsylvania Turnpike	8.4	Aug. 12, 5:10 P.M.	29.91	33.5	Cove Valley Service Area
8.	Pittsburgh, Pa.	9.8	Aug. 13, 9:10 A.M.	29.44	20.5	712 Middle Street, corner of Emlin and Middle, residential
9.	Pittsburgh, Pa.	11.6	Aug. 13, 11:00 A.M.	29.16	23.4	Corner of Harper and Evergreen, suburban residential street, Northwest Pittsburgh
10.	Pittsburgh, Pa.	13.9	Aug. 13, 11:15 A.M.	29.05	23.4	Corner of Perrymont Road and McKnight, 8 miles Northwest of City
11.	Ohio Turnpike	12.0	Aug. 13, 1:00 P.M.	28.99	29.6	Portage Service Area

LOCATION	RADIATION LEVEL (μr/hr)	DATE AND TIME (1957)	PRESSURE (Inches)	TEMPERATURE (^{o}C)	COMMENTS
12. Cleveland, Ohio	11.8	Aug. 13, 2:30 P. M.	29.30	29.5	7514 Stone Rd., suburb of Cleveland near intersection of Stone Road and US 21
13. Cleveland, Ohio	10.5	Aug. 13, 3:00 P.M.	29.52	32.5	Corner of Huron and Ontario
14. Ohio Turnpike	11.6	Aug. 13, 4:25 P.M.	29.39	31.0	Middle Ridge Plaza between Cleveland and Toledo
15. Toledo, Ohio	10.0	Aug. 13, 6:55 P.M. (EDT) 5:55 P.M. (EST)	29.47	34.0	2935 Jerusalem Road, Swartz Motel, 4.5 miles east of Toledo on Route 2.
16. Toledo, Ohio	14.9	Aug. 13, 6:10 P.M.	29.49	31.4	Monroe and Water Street, downtown; over Granite Paving Stone
17. Toledo, Ohio	8.7	Aug. 13, 6:50 P.M.	29.44	29.2	4535 Monroe, Parking Lot of Tivoli Restaurant
18. Ohio Turnpike	9.5	Aug. 14, 7:45 A.M.	29.33	26.5	Oak Openings Plaza; approx. 30 miles west of Toledo
19. Indiana Turnpike	9.6	Aug. 14, 10:45 A.M.	29.18	27.0	Wilbur Shaw Service area, approx. 75 miles east of Chicago
20. Chicago, Illinois	10.6	Aug. 14, 12:35 P.M.	29.46	28.7	S. Ave. L and E. 98 Street Residential street
21. Chicago, Illinois	11.6	Aug. 14, 12:55 P.M.	29.45	30.4	S. Coles Ave. and E. 78 St. near St. Brides School
22. Chicago, Illinois	10.7	Aug. 14, 1:10 P.M.	29.45	30.8	Jackson Park near Lake Michigan

	LOCATION	RADIATION LEVEL (μr/hr)	DATE AND TIME (1957)	PRESSURE (inches)	TEMPERATURE (°C)	COMMENTS
23.	Chicago, Illinois	17.0	Aug. 14, 1:45 P. M.	29.43	31.5	65 West Adams; adjacent to U.S. Post Office of Granite Construction; near intersection with Clark
24	Chicago, Illinois	10 3	Aug. 14, 3:15 P.M.	29.38	35.1	Midway Airport; Parking Lot 5036 W. 63 Street
25.	Lake Geneva, Wisconsin	8.5	Aug. 14, 6:40 P.M.	29.11	29.6	Center of Town; outside First National Bank
26	Whitewater, Wisconsin	9.0	Aug. 14, 7:30 P. M.	29.17	27.0	Residential Street
27	Madison, Wisconsin	10.4	Aug. 14, 11:00 P.M	29.08	26.3	Pinckney and Washington; opposite State Capitol
28	Madison, Wisconsin	10.3	Aug. 14, 11:30 P.M.	29.15	24.0	Motel Madison; Junction Route 51 and Route 12; approx. 8 miles east of Madison
29.	Madison, Wisconsin	10.1	Aug. 15, 8:15 A.M.	29.08	25.0	Approx. 5 miles east of Madison on Route 12
30.	Richland Center, Wis.	9.6	Aug. 15, 9:30 A.M.	29.24	23.5	Corner of East Haseltine and Church Street
31.	La Crosse, Wisconsin	9.6	Aug. 15, 11:05 A.M.	29.36	29.0	Cass and 3rd Street near bridge over Mississippi River
32.	Winona, Minnesota	10.1	Aug. 15, 12 Noon	29.40	30.1	Parking Lot of Hot Fish Shop Restaurant

LOCATION	RADIATION LEVEL (μr/hr)	DATE AND TIME (1957)	PRESSURE (inches)	TEMPERATURE (°C)	COMMENTS
33. Winona, Minnesota	12.0	Aug. 15, 12:55 P. M.	29.40	35.0	Intersection of Belleview and Carimona; Residential
34. Red Wing, Minnesota	11.1	Aug. 15, 2:45 P. M.	29.39	32.7	Intersection of 3rd St. and Plum; downtown
35. St. Paul, Minnesota	12.4	Aug. 15, 4:00 P. M.	29.29	28.5	On Hastings; near intersection of Maria and Wilson
36. St. Paul, Minnesota	11.1	Aug. 15, 4:25 P.M.	29.35	31.0	Robert St., near 9th St. downtown
37. Minneapolis, Minnesota	9.1	Aug. 15, 5:15 P.M.	29.30	30.2	Intersection 2 St. and Third Avenue, downtown; adjacent to Federal Office Building
38. Minneapolis, Minnesota	12.5	Aug. 15, 6:15 P. M.	29.24	30.4	Intersection, West 41st St. and Vernon; Residential
39. Le Sueur, Minnesota	10.9	Aug. 15, 7:30 P.M.	29.37	27.5	Near Downtown; Intersection of N. Main and Swan; latter a Residential Street
40. Worthington, Minnesota	14.7	Aug. 16, 9:30 A.M.	28.67	23.8	Intersection Grand and Dover, Residential
41. Luverne, Minnesota	13.6	Aug. 16, 10:45 A.M.	28.79	25.3	Freeman Street near Cedar St.
42. Sioux Falls, South Dakota	11.8	Aug. 16, 11:35 A.M.	28.83	31.0	Intersection 10th St. and Phillips Ave., Downtown
43. Sioux Falls, South Dakota	11.5	Aug. 16, 11:50 A.M.	28.75	29.7	Intersection West 10th St. and S. Euclid Ave., Resid.

LOCATION	RADIATION LEVEL (μr/hr)	DATE AND TIME (1957)	PRESSURE (inches)	TEMPERATURE (^{o}C)	COMMENTS
44. Mitchell, South Dakota	11.1	Aug. 16, 1:20 P.M. (CDT) 12:20 P.M. (CST)	28.92	34.7	Intersection of Main Street and First Ave. Downtown
45. Chamberlain, South Dakota	11.3	Aug. 16, 2:55 P.M.	28.76	32.5	Junction U.S. 16 and S.D. 47
46. Presho, South Dakota	11.1	Aug. 16, 4:05 P.M.	28.35	31.9	On U.S. 16, Frontier Gas Station
47. Murdo, South Dakota	13.4	Aug. 16, 4:55 P.M.	27.78	30.1	Unmarked, unpaved residential street, one block north of U. S. 16
48. Kadoka, South Dakota	14.1	Aug. 16, 6:05 P.M. (CST) 7:05 P.M. (CDT) 5:05 P.M. (MST)	27.62	31.0	Silver Court Motel, 2 blocks south of U.S. 16; Residential
49. Kadoka, South Dakota	15.1	Aug. 17, 6:15 A.M.	27.67	21.3	Same as Position 48. Difference possibly attributable to car loading.
50. Badlands, South Dakota	16.5	Aug. 17, 7:00 A. M.	27.61	25.0	Entrance to Badlands
51. Badlands, South Dakota	17.3	Aug. 17, 8:30 A.M.	27.67	29.5	Heart of Badlands
52. Wall, South Dakota	14.3	Aug. 17, 10:15 A.M.	27.33	26.4	Center of Town
53. Rapid City, South Dakota	14.4	Aug. 17, 11:45 A.M.	26.97	23.6	On 6th St. between Main and St. Joseph; downtown
54. Keystone, South Dakota	33.8	Aug. 17, 1:00 P. M.	27.85	24.4	In Black Hills on U.S. 16 A. Resurvey on Sept. 19 indicates elevated background principally attributable to fallout.

RELATIVE ACTIVITY OF BUILDING BRICKS

COUNTS/SECOND whole brick counter NaI Scintillator (P)

LOCATION	TYPE	HIGH ABSORPTION		MEDIUM ABSORPTION		LOW ABSORPTION		UNCLASSIFIED
Salisbury, North Carolina	--	62	65	68	68	72	72	48, 48, 49, 49, 51, 59
Atlanta, Georgia	Surface Clay	82	83	98	104	94	87	
Canton, Ohio	Fire Clay							125, 125, 128, 128
" "	Shale							89, 99
Columbus, Ohio	--							86, 86, 89, 89, 92, 92
Streator, Illinois	Shale	76	78	77	76	80	79	
Chicago, Illinois	--							72, 73, 74, 74, 75, 78
Danville, Illinois	Fire Clay	91	97	103	100	119	119	
Fairbury, Nebraska	Fire Clay	69	68	67	67	68	68	
Denver, Colorado	Shale and Surface Clay	86	60			76	93	
" "	Surface Clay			96	96			
" "	Surface Clay	111	111	111	134	96	96	
" "	Fire Clay	135*	144*	165	165	388*	370*	
" "	Fire Clay	236	236	214	214	191	184	
Wichita, Kansas	Surface Clay							71, 82, 82, 137, 140, 166
Austin, Texas	--							59, 59, 60, 63, 65, 65, 93, 97, 97, 99, 104, 107
San Francisco, California	--							39, 46, 48, 52, 53, 55, 56, 65, 71, 80, 84 (**)
New York, New York	--							68, 70, 70, 71, 72

BACKGROUND: APPROXIMATELY 12 C/SEC.

NOTE: * *These bricks are 1 to 3 pounds heavier than the average brick which weighs about 5 pounds.*

** *These bricks averaged about 6 pounds in weight.*

LOCATION	RADIATION LEVEL (μr/hr)	DATE AND TIME (1957)	PRESSURE (inches)	TEMPERATURE (°C)	COMMENTS
55. Black Hills, South Dakota	22.0	Aug. 17, 1:30 P. M.	25.1	24.0	Mount Rushmore, Observation Point; parking field
56. Black Hills, South Dakota	24.6	Aug. 17, 2:45 P. M.	26.0	28.0	State Game Lodge; See comment, Position 54
57. Custer, South Dakota	16.3	Aug. 17, 4:30 P.M.	25.0	26.5	Adjacent to U.S. Post Office
58. Hot Springs, South Dakota	15.3	Aug. 17, 5:45 P.M.	26.67	25.7	Adjacent to City Auditorium
59. Lusk, Wyoming	15.1	Aug. 17, 8:30 P.M.	25.28	24.0	Corner of W. 3rd St. and Barrett Boulevard; adjacent to Lusk Cabin Court.
60. Lusk, Wyoming	16.1	Aug. 18, 7:00 A. M.	25.25	13.7	Same as Position 59. See comment Position 49.
61. Lingle, Wyoming	16.7	Aug. 18, 9:20 A.M.	26.06	23.3	1 block east of Main St. on U. S. 85
62. Torrington, Wyoming	17.6	Aug. 18, 9:45 A.M.	26.11	23.7	Center of Town, Opposite Trail Hotel and Citizens National Bank
63. Cheyenne, Wyoming	17.2	Aug. 18, 11:45 A.M.	24.30	27.4	On Central Ave. Near First Ave. West, residential
64. Cheyenne, Wyoming	17.6	Aug. 18, 12:20 P.M.	24.51	30.5	Adjacent to Wyoming State Capitol Building, E. 24th St. near Central Avenue
65. Denver, Colorado	17.7	Aug. 18, 2:55 P.M.	25.02	33.6	Approx. 15 miles north of Denver on US 87, Approx. 100 feet north of intersection with Bull Canal

LOCATION	RADIATION LEVEL (μr/hr)	DATE AND TIME (1957)	PRESSURE (inches)	TEMPERATURE (^{o}C)	COMMENTS
66. Denver, Colorado	18.1	Aug. 18, 4:05 P. M.	24.85	32.5	On Evans near Fillmore
67. Denver, Colorado	19.4	Aug. 18, 5:05 P. M.	24.95	32.9	Carport of Royal Motel, intersection of South Broadway and Iowa Avenue
68. Denver, Colorado	18.0	Aug. 18, 5:30 P.M.	24.98	32.6	Intersection of Raritan and Nevada; residential
69. Denver, Colorado	17.4	Aug. 18, 5:45 P.M.	24.97	32.4	Intersection of Santa Fe Drive, West eighth Avenue; Shopping area
70. Denver, Colorado	22.4	Aug. 18, 6:00 P. M.	24.97	32.5	On Cherokee St. between 14 St. and Colfax between U.S Mint and City & County Building.
71. Denver, Colorado	18.9	Aug. 18, 6:30 P.M.	24.99	30.8	East corner of Wilton and 23rd St., near downtown
72. Denver, Colorado	16.6	Aug. 18, 6:45 P.M.	25.03	31.3	Near 18th St. & Wyncoop in Union Station Parking Lot
73. Denver, Colorado	17.6	Aug. 18, 7:10 P.M.	24.94	30.5	Intersection of 38th Ave. and Tejon
74. Denver, Colorado	18.4	Aug. 18, 7:45 P.M.	24.93	27.2	Adjacent to Denver Museum of Natural History
75. Denver, Colorado	17.9	Aug. 18, 8:00 P.M.	24.85	28.6	Intersection of 7th Ave. and Monroe, residential

LOCATION	RADIATION LEVEL (μr/hr)	DATE AND TIME (1957)	PRESSURE (inches)	TEMPERATURE (^{o}C)	COMMENTS
76. Denver, Colorado	19.9	Aug. 19, 9:20 A.M.	24.31	32.3	On U.S. 85, approximately 44 miles north of Colorado Springs, Colorado
77. Colorado Springs, Colorado	19.3	Aug. 19, 10:45 A.M.	24.22	33.0	Intersection of East Madison and North Nevada; residential
78. Colorado Springs, Colorado	22.3	Aug. 19, 11:25 A.M.	24.30	32.8	Kiowa Ave. between Cascade and Tejon; downtown
79. Colorado Springs, Colorado	20.7	Aug. 19, 12:30 P.M.	24.25	33.4	Vermijo at 23rd Street; unpaved residential street
80. Pikes Peak Highway, Col.	26.6	Aug. 19, 1:00 P.M.	22.97	33.5	One mile beyond Cascade, Colorado
81. Pikes Peak Highway, Col.	35.0	Aug. 19, 1:40 P.M.	21.28	30.5	Halfway Water Station, actual altitude, 9,950 feet
82. Pikes Peak Summit, Col.	38.6	Aug. 19, 3:00 P.M.	18.46	34.0	Actual altitude 14,110 feet
83. Colorado Springs, Col.	20.3	Aug. 20, 6:05 A.M.	24.12	16.0	Town House Motel Parking Lot
84. Hartsel, Colorado	23.9	Aug. 20, 9:10 A. M.	22.03	24.0	Sand & Gravel Parking lot of Holiday Inn Hotel
85. Buena Vista, Colorado	24.5	Aug. 20, 10:10 A.M.	22.50	25.0	Near intersection, US 24 and Colorado 306
86. Leadville, Colorado	23.5	Aug. 20, 11:10 A.M.	21.10	25.4	Center of Town, East 6th St. near Harrison; unpaved
87. Glenwood Springs, Col.	17.1	Aug. 20, 3:10 P.M.	24.52	23.0	Intersection of Grand Avenue and Eighth Street; downtown

LOCATION	RADIATION LEVEL (μr/hr)	DATE AND TIME (1957)	PRESSURE (inches)	TEMPERATURE (°C)	COMMENTS
88. Rifle, Colorado	17.3	Aug. 20, 5:10 P. M.	24.87	25.0	On East 3rd Street just west of White River Avenue; residential, one block from business district
89. Grand Junction, Col.	15.7	Aug. 20, 7:15 P. M.	25.47	27.2	Intersection Cannell and Glenwood, residential, outside Calvary Bible Church
90. Grand Junction, Col.	16.6	Aug. 21, 7:10 A. M.	25.54	20.0	Lazy Bar X Motel driveway
91. Grand Junction, Col.	18.4	Aug. 21, 9:30 A.M.	25.60	24.7	Outside AEC Operations Office
92. Colorado Plateau, Col.	16.5	Aug. 21, 12:00 Noon	23.54	29.0	Between towns of Whitewater and Gateway Unaweep Canyon, approximately 25 miles south of Whitewater
93. Colorado Plateau, Col.	16.4	Aug. 21, 1:05 P. M.	25.30	24.8	Approx. two miles north of Gateway
94. Moab, Utah	14.7	Aug. 21, 6:20 P. M.	25.98	31.8	Outside, 160 Main Street, downtown
95. Monticello, Utah	16.9	Aug. 21, 8:30 P. M.	23.50	23.8	Adjacent to Hills Triangle Motel
96. Monticello, Utah	16.9	Aug. 22, 7:40 A. M.	23.54	18.0	Same as Position 95
97. Dove Creek, Colorado	19.1	Aug. 22, 8:35 A.M.	23.72	24.2	On unpaved portion on US 160 in construction area
98. Cortez, Colorado	15.5	Aug. 22, 9:35 A. M.	24.29	27.0	Center of town; off pavement

	LOCATION	RADIATION LEVEL (μr/hr)	DATE AND TIME (1957)	PRESSURE (inches)	TEMPERATURE (°C)	COMMENTS
99.	Navajo Indian Reservation, New Mexico	17.6	Aug. 22, 11:30 A. M.	25.12	32.4	—
100.	Shiprock, New Mexico	16.5	Aug. 22, 12:00 Noon	24.97	34.8	—
101.	Buffalo Springs Trading Post, New Mexico	20.3	Aug. 22, 1:30 P. M.	24.33	33.2	On US 666 between towns Gallup and Naschitti
102.	Gallup, New Mexico	18.5	Aug. 22, 2:40 P. M.	23.95	33.2	On East 66th St. near First Avenue, downtown
103.	Grants, New Mexico	15.5	Aug. 22, 5:15 P. M.	23.94	29.0	Outskirts over unpaved ground adjacent to trailer camp
104.	Grants, Nex Mexico	13.8	Aug. 22, 5:35 P. M.	23.98	29.5	"Downtown", on paved US 66
105.	Albuquerque, New Mexico	14.1	Aug. 23, 6:45 A.M.	25.30	22.4	Monterey Court Parking area, west side of City, off US 66
106.	Albuquerque, New Mexico	14.4	Aug. 23, 7:20 A. M.	25.30	23.6	"Old City", adjacent to Church of San Felipe de Neri
107.	Albuquerque, New Mexico	13.8	Aug. 23, 7:45 A. M.	25.29	25.0	Intersection of Central Ave. and Fourth Street; downtown
108.	Albuquerque, New Mexico	14 5	Aug. 23, 8:30 A. M.	25.13	30.6	West side near Trinity Methodist Church off U. S. 66
109.	Albuquerque, New Mexico	15.2	Aug. 23, 10:00 A. M.	24.14	26.1	"Open Country" between Albuquerque and Santa Rosa, approximately 43 miles west of Santa Rosa, across from Standard Asphalt Plant.

LOCATION	RADIATION LEVEL (μr/hr)	DATE AND TIME (1957)	PRESSURE (inches)	TEMPERATURE (°C)	COMMENTS
110. Santa Rosa, New Mexico	12.9	Aug. 23, 11:15 A. M.	25.60	30.0	Adjacent to Santa Rosa Town Hall on U. S. 66
111. Tucumcari, New Mexico	13.1	Aug. 23, 12:40 P.M. (MST) 1:40 P.M. (CST)	26.06	31.5	Intersection; E. Hines Ave. and S. First Ave., residential street one block from U. S. 66
112. Amarillo, Texas	15.0	Aug. 23, 3:20 P. M.	26.22	33.5	Between Tucumcari, New Mexico and Amarillo, Texas, approximately 65 miles west of Amarillo over red soil on plains
113. Amarillo, Texas	13.3	Aug. 23, 4:45 P. M.	26.39	34.2	W. edge of town, Ranch 66 Motel
114. Amarillo, Texas	12.9	Aug. 24, 8:15 A.M.	26.36	23.9	Same as Position 113
115. Amarillo, Texas	13.6	Aug. 24, 10:00 A.M.	26.40	26.0	Intersection, south Filmore Street and East 6th Avenue; downtown
116. Amarillo, Texas	13.4	Aug. 24, 10:15 A.M.	26.39	27.6	Intersection NE 7th Avenue and North Pierce, Residential
117. McLean, Texas	13.1	Aug. 24, 11:50 A.M.	27.12	29.2	One block North of U.S. 66 and one block West of Main Street; residential
118. Sayre, Oklahoma	11.0	Aug. 24, 1:15 P.M.	28.11	32.0	Downtown, outside City National Bank

LOCATION	RADIATION LEVEL (μr/hr)	DATE AND TIME (1957)	PRESSURE (inches)	TEMPERATURE (^{o}C)	COMMENTS
119. Elk City, Oklahoma	11.8	Aug. 24, 2:25 P.M.	27.93	36.0	Unpaved parking lot off US 60 near center of town
120. Clinton, Oklahoma	14.5	Aug. 24, 3:05 P.M.	28.33	34.5	Intersection of Knox and S. 7th St. Paved residential street
121. Clinton, Oklahoma	12.5	Aug. 24, 3:25 P.M.	28.36	34.8	Intersection of Frisco Ave. and North Fourth St.
122. El Reno, Oklahoma	10.0	Aug. 24, 4:55 P.M.	28.54	32.8	Downtown on U.S. 66, adjacent to Sacred Heart Academy
123. Oklahoma City, Oklahoma	10.5	Aug. 24, 5:45 P.M.	28.65	32.7	Corner of 22 St. and North Ross; residential
124. Oklahoma City, Oklahoma	10.5	Aug. 24, 6:10 P.M.	28.69	33.1	On 3 St. between Harvey & Robinson adjacent to U. S. Post Office; downtown
125. Oklahoma City, Oklahoma	9.9	Aug. 24, 6:40 P.M.	28.67	33.2	In front of State Capitol Building, NE 23 St. and Lincoln Boulevard
126. Oklahoma City, Oklahoma	10.5	Aug. 24, 6:50 P.M.	28.73	33.4	NE section of City on red dirt road just west of Lincoln Boulevard in close proximity to oil fields.
127. Tulsa, Oklahoma	11.6	Aug. 25, 7:35 A.M.	29.23	22.0	6 miles west of City, Winston's Motor Court.
128. Tulsa, Oklahoma	11.6	Aug. 25, 9:30 A.M.	29.38	31.0	SW Boulevard and W. 21 Street

	LOCATION	RADIATION LEVEL (μr/hr)	DATE AND TIME (1957)	PRESSURE (inches)	TEMPERATURE (°C)	COMMENTS
129.	Tulsa, Oklahoma	11.1	Aug. 25, 9:55 A. M.	29.28	32.3	Fourth St. and South Main, one block from City Hall, downtown
130.	Tulsa, Oklahoma	10.8	Aug. 25, 10:20 A. M.	29.28	32.8	On East 14th St. between Rockford and St. Louis Avenues; residential
131.	Muskogee, Oklahoma	18.6	Aug. 25, 11:45 A. M.	29.39	34.7	Okmulgee Street near S. 26 Street; residential
132.	Muskogee, Oklahoma	14.1	Aug. 25, 12:05 P. M.	29.39	35.5	Intersection of West Okmulgee St. and N. 4th St. downtown
133.	Muskogee, Oklahoma	14.1	Aug. 25, 12:20 P. M.	29.41	36.2	South B and Kalamazoo over dirt road
134.	Fort Smith, Arkansas	17.0	Aug. 25, 2:20 P. M.	29.55	38.3	On North 6th Street between Rogers and Parker, between U. S. Post Office and County Building, downtown
135.	Fort Smith, Arkansas	14.1	Aug. 25, 2:35 P. M.	29.55	37.2	Intersection of North 13 St. and N. A St., across from First Christ Church, edge of downtown section
136.	Russellville, Arkansas	16.6	Aug. 25, 5:25 P. M.	29.65	33.6	Intersection of Main and Commerce on Main, center of town
137.	Russellville, Arkansas	13.6	Aug. 25, 5:45 P. M.	29.65	34.3	East 5th St. & S. Cleveland; residential

	LOCATION	RADIATION LEVEL (μr/hr)	DATE AND TIME (1957)	PRESSURE (inches)	TEMPERATURE (^{o}C)	COMMENTS
138.	Little Rock, Arkansas	13.3	Aug. 25, 8:00 P. M.	29.72	29.7	West 3 St. and S. Arch, near downtown, residential area adjacent
139.	Little Rock, Arkansas	12.8	Aug. 25, 8:20 P. M.	29.72	31.2	Near base of steps of new State Capitol Building off W. 3rd Street
140.	Hazen, Arkansas	26.0	Aug. 25, 9:55 P. M.	29.85	26.3	Outside Proctor's Esso Station. Resurvey on Sept. 5 indicate elevated radiation level principally attirbutable to fallout
141.	Brinkley, Arkansas	30.8	Aug. 26, 8:05 A. M.	30.04	29.2	On gravelled parking lot of Rusher Motel; see comment, position 140
142.	Brinkley, Arkansas	24.8	Aug. 26, 9:35 A.M.	30.04	30.5	Intersection of Cypress and New Orleans downtown, see comment, postion 140
143.	Wheatley, Arkansas	50.2	Aug. 26, 10:00 A. M.	30.03	33.5	On reddish gravel off Route 70 near stores. See comment, position 140
144.	Forrest City, Arkansas	12.2	Aug. 26, 11:00 A. M.	29.96	32.6	Washington Ave. (U.S. 70) one block west of Junction Arkansas, downtown
145.	Memphis, Tennessee	11.0	Aug. 26, 12:15 P. M.	29.95	34.9	Intersection Court Ave. and N. Front Street near U. S. Post Office, one block from Mississippi River, downtown

LOCATION	RADIATION LEVEL (μr/hr)	DATE AND TIME (1957)	PRESSURE (inches)	TEMPERATURE (°C)	COMMENTS
146. Memphis, Tennessee	9.4	Aug. 26, 12:45 P. M.	29.59	35.8	Intersection of Adams - N. Third Street; downtown
147. Memphis, Tennessee	13.3	Aug. 26, 1:15 P. M.	29.91	36.6	Intersection of Poplar and Auberndale St., near brick apartment house, residential
148. Corinth, Mississippi	11.6	Aug. 26, 3:30 P. M.	29.71	33.0	Southern outskirts of town unpaved parking lot of Kathy's Restaurant
149. Decatur, Alabama	14.3	Aug. 26, 6:25 P. M.	29.55	30.2	Intersection of Bank and Church Street, downtown. Strip of brick paving on edge of road exhibited extremely high activity contributing to somewhat elevated background.
150. Decatur, Alabama	13.1	Aug. 26, 6:40 P. M.	29.59	31.2	Intersection of NE Oak and Church Streets; residential
151. Huntsville, Alabama	11.7	Aug. 26, 7:35 P.M. (CST) 6:35 P.M. (EST)	29.55	29.2	On Holmes Street, 5 blocks west of downtown area near bus station and Church of Nazarene; residential
152. Chattanooga, Tennessee	14.8	Aug. 27, 7:00 A. M.	29.50	18.0	Western outskirts of City, sand and gravel parking lot of Turner's Auto Court off U. S. 72. Brick facing of motel units exhibited somewhat elevated activities.

LOCATION	RADIATION LEVEL (μr/hr)	DATE AND TIME (1957)	PRESSURE (inches)	TEMPERATURE (°C)	COMMENTS
153. Chattanooga, Tennessee	16.1	Aug. 27, 9:20 A. M.	29.59	28.2	On 8th St. between Broad and Market, narrow street with stores and offices; downtown
154. Chattanooga, Tennessee	11.1	Aug. 27, 9:45 A. M.	29.59	30.0	Outside 921 Market near 10th Street, wide business thoroughfare, downtown
155. Chattanooga, Tennessee	12.3	Aug. 27, 10:00 A. M.	29.57	30.9	Intersection of West Duncan and South Kelly; residential

APPENDIX II

Instrumentation

In this appendix are described the instrument and the technique of measurement. As mentioned in the main portion of this paper, measurements were made with a 20-liter ionization chamber filled with air at atmospheric pressure. The instrument was operated inside an automobile under essentially identical conditions of vehicle loading and orientation. The ionization current was measured with a vibrating reed electrometer connected as a continuously reading voltmeter driving a pen recorder. Power for the electrometer and recorder was obtained from an alternating current inverter operated from the 12-volt automobile storage battery. The entire assembly was secured to a wooden carrying board as shown in the photograph (Fig. II-1).

The chamber was improvised from a 20-liter polyethylene carboy having a 3/32-inch wall. To suppress completely the beta response, the chamber was positioned in a solid 1/8-inch aluminum shield. Including the polyethylene wall, the gas volume was enclosed by 1.08 g/cm^2 of material, corresponding to the Feather range of a 2.26 Mev beta particle.

A schematic diagram of the ionization chamber showing the details of the center electrode assembly is shown in Figure II-2.

The chamber has two guard rings with the top of the center electrode secured by the guard ring assembly to the carboy. The top and bottom guard rings are connected together by an insulated wire strung through the stainless steel electrode. For laboratory use one could dispense with the top assembly but for field use the additional mechanical rigidity is advantageous. There is sufficient air leakage in the chamber so that the chamber maintains atmospheric pressure. This was verified in the field by checking the response of the chamber to a weak source against the known barometric pressure.

As is well known, minute alpha contamination of an ionization chamber at atmospheric pressure can produce a current which may be of the same order as the current being measured. For this reason it is essential that the effect of contamination be measured or that the current produced by alpha particles be suppressed. A method of evaluating the alpha current is furnished by Hess and Vancour.[a] Essentially, the method depends on the limited range of alpha particles resulting in the alpha-produced ionization being independent of the pressure, whereas the ionization produced by gamma radiation (or charged relativistic particles in the cosmic radiation) is almost exactly proportional to the pressure.

A frequently used procedure is to pressurize the chamber filling (usually purified argon) so that the alpha contribution is negligible compared to the ionization produced by an external radiation field.

In our measurements we devised a different technique more suited to our facilities which depends on the difference in electric fields necessary to effect total collection of ion pairs produced by particles of low and high specific ionization; i.e., electrons from gamma-ray and alpha-particle interactions respectively.

Figure II-3 shows an ion collection characteristic for two different radiation fields measured with our apparatus. The upper curve is for an external field of 215 microroentgens/hour from a radium source at a distance of several meters from the chamber. The lower curve is for the radiation background for the same position in the Health and Safety Laboratory. During this measurement the background was about eight microroentgens/hour. It can be seen that for the elevated radiation field the saturation potential is reached with a collecting potential of 20 volts across the chamber. On the other hand, for the background curve, where the saturation collecting potential must be less than that required for the higher radiation field, the characteristic shows a pronounced rise from 50 to 300 volts. This rise follows a plateau between 10 and 50 volts. At 300 volts the measured ionization current is more than fifty percent greater than the ionization current in the 10- to 50-volt interval. Figure II-4, which plots the fraction of the ion current at 300 volts against the collecting potential, shows this effect more graphically.

The explanation for this is simple. While saturation for the ionization produced by gamma rays is quickly achieved, collection for the alpha ionization is relatively inefficient and in fact saturation is not reached up to the maximum collecting potential used. The important feature of the curves shown in Fig. II-3 and Fig. II-4 is that for a considerable range in collecting potential, up to about fifty volts, the alpha contribution is suppressed to the point where it makes a negligible contribution to the total ion current. This situation prevails provided one reads the minimum envelope of the output trace.

The character of the trace obtained with different collecting potentials is shown in Fig. II-5. The figure shows the trace of the electrometer zero (A), the trace with no collecting potential applied to the chamber (B), and the background trace with the different collecting potentials up to 300 volts (C). One may observe the alpha pulses becoming more prominent as the collecting potential is increased. The saturation curves previously described were taken at the lower envelope or minima of these traces. When runs are made over an extended period (of the order of ten or more minutes) minima occur with the same amplitude. One infers that these minima are associated with the absence of ionization caused by alpha particles.

The general behavior of the phenomena described can be interpreted in terms of the Jaffé-Zanstra theory of columnar recombination.[b] However, the theory is not sufficiently precise to furnish much more than a qualitative description of the difference in saturation characteristics for radiations of different specific ionizations in air-filled chambers.

Calibration and Measurement Procedure

Calibration of the ionization chamber is done with a 1.021 milligram radium source in an 0.2 mm wall platinum needle. The needle is placed in an aluminum source holder 1.8 mm thick. The radium equivalent of this needle has been determined by the National Bureau of Standards and a value of 0.84 rhm has been taken for the dose rate output[c] of the radium. The source is positioned 2 meters away from the geometric center of the chamber and the dose rate estimated by simple inverse square. No correction has been made for the absorption of the air between the source and chamber which is perhaps slightly overcompensated by scatter from walls, floors, and neighboring objects in the laboratory.

After zeroing the electrometer, the chamber is operated with no collecting potential. The resulting trace varies in value from zero to a reading corresponding to about fifty percent of the laboratory background. The reading is generally stable for very long periods. When it changes, it does so with a time constant measured in hours. It is radiation sensitive but to an extent which is less than one percent of the calibration sensitivity of the chamber with collecting potential, and in the opposite direction. The precise behavior of this spurious current is complex though we find that a new chamber, having an aquadag coated lucite center electrode, does not exhibit this "zero" current to the same extent. It is probably identical to what Ohmart has called the "radioelectric effect."[d]

After the zero reading, a 22.5-volt collecting potential is applied and the background reading determined. A background trace is taken for approximately five minutes. The difference between the zero and background readings constitute the required measurement.

A calibration factor for the chamber of 0.498 $\frac{\mu r/hr}{mv}$ (STP) or 2.09×10^{-15} $\frac{\text{amperes}}{\mu r/hr}$ has been obtained. The latter value depends, of course, on the correctness of the glass-sealed Victoreen resistor used in conjunction with the vibrating reed electrometer. The value of the resistor used in these measurements was 9.6×10^{11} ohms as furnished by the manufacturer and verified in this laboratory. Using the roentgen as equivalent to 1 esu/cm^3, one obtains the easy conversion that 1 μr/hr is equivalent to 0.576 ion pairs/cm^3-sec. With the calibration factor above, this corresponds to a sensitive volume of 22.7 liters in reasonable agreement with the geometrical volume of 21.3 liters. Because of wall effects, ionization chamber theory would predict only an approximate equality between geometric and ionization volumes.

Because of the substantially isotropic nature of the radiation measured, an alternative and possibly superior method of calibration is to position the source in a number of points around the chamber and average the calibration factors so obtained. This method of calibration would correct in some measure for the shielding of terrestrial radiation furnished by the components surrounding the ion chamber, but also would result in an overestimation of the cosmic-ray contribution which is not shielded significantly by the surrounding apparatus. At this stage in our work we do not feel that this degree of refinement in the calibration constant is indicated considering the grosser errors inherent in field measurements of this type.

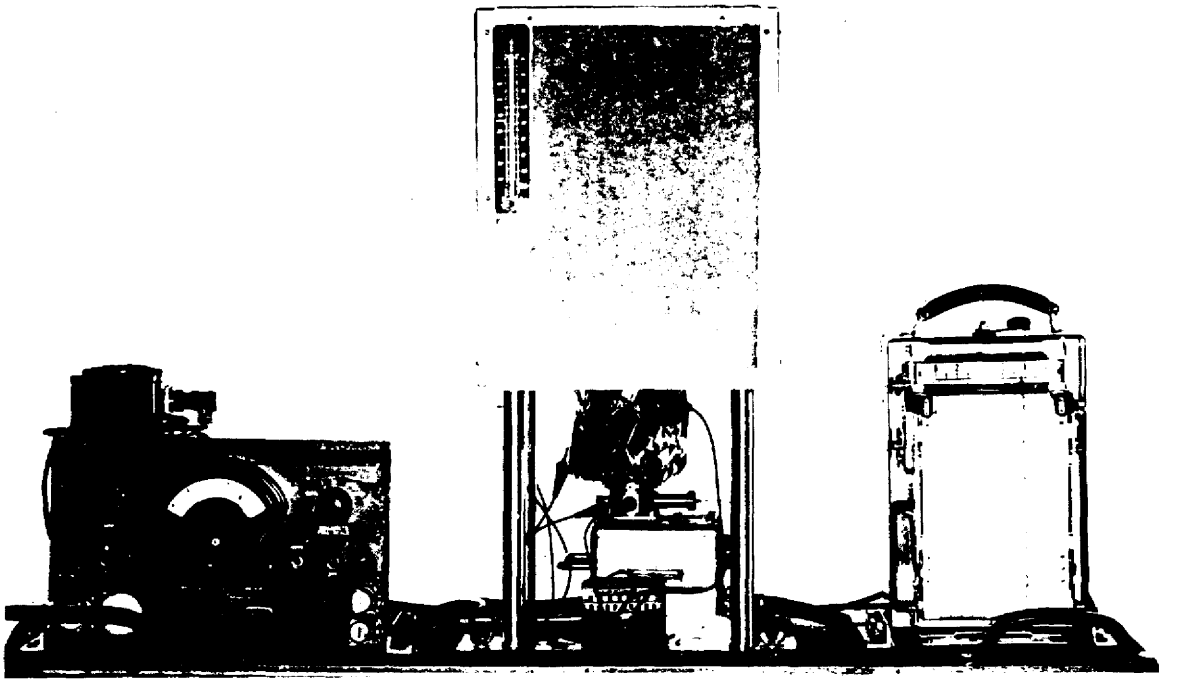

TWENTY LITER IONIZATION CHAMBER
AND ASSOCIATED APPARATUS

FIGURE II-1

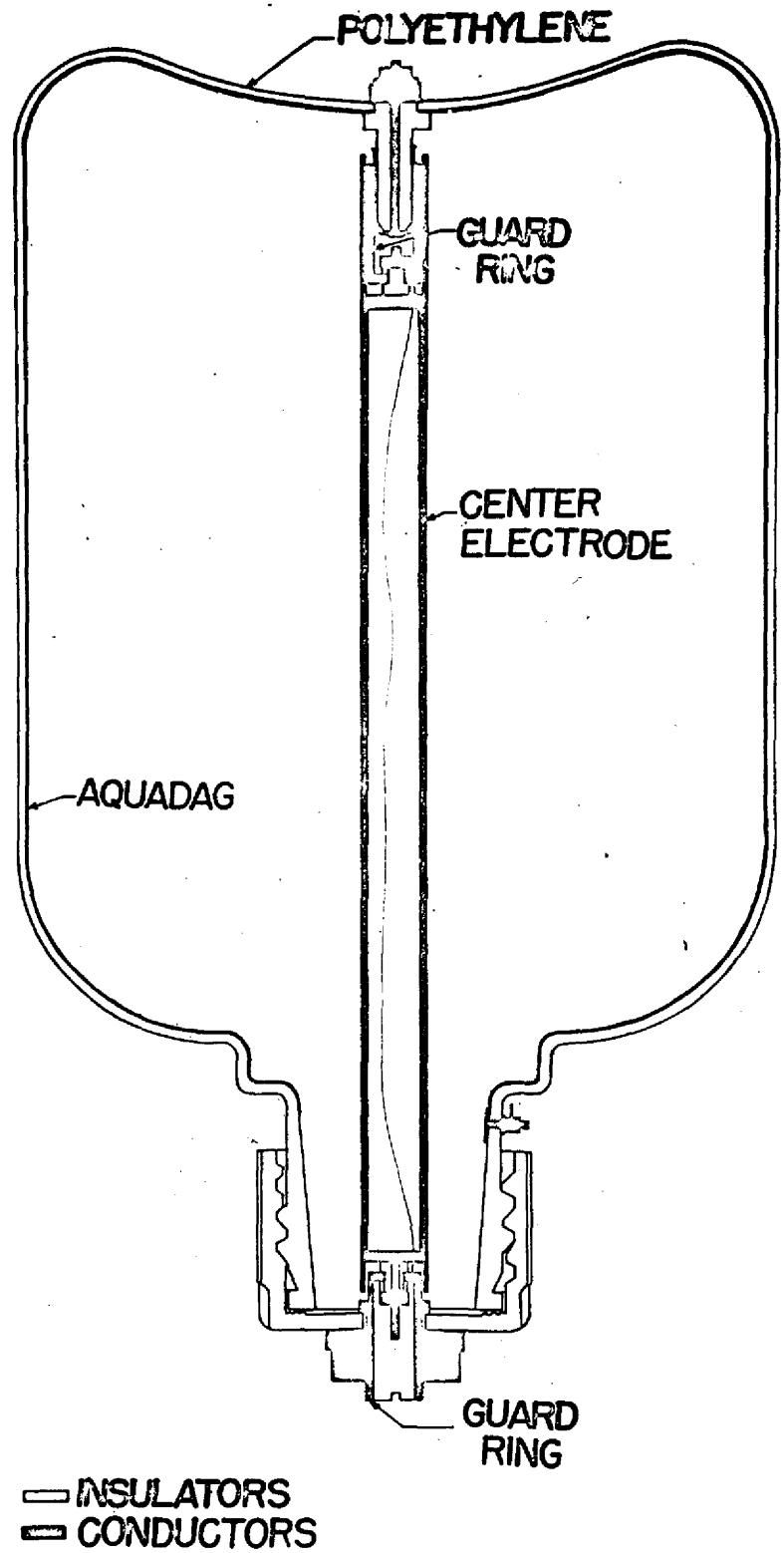

Twenty Liter Ionization Chamber

Figure II-2

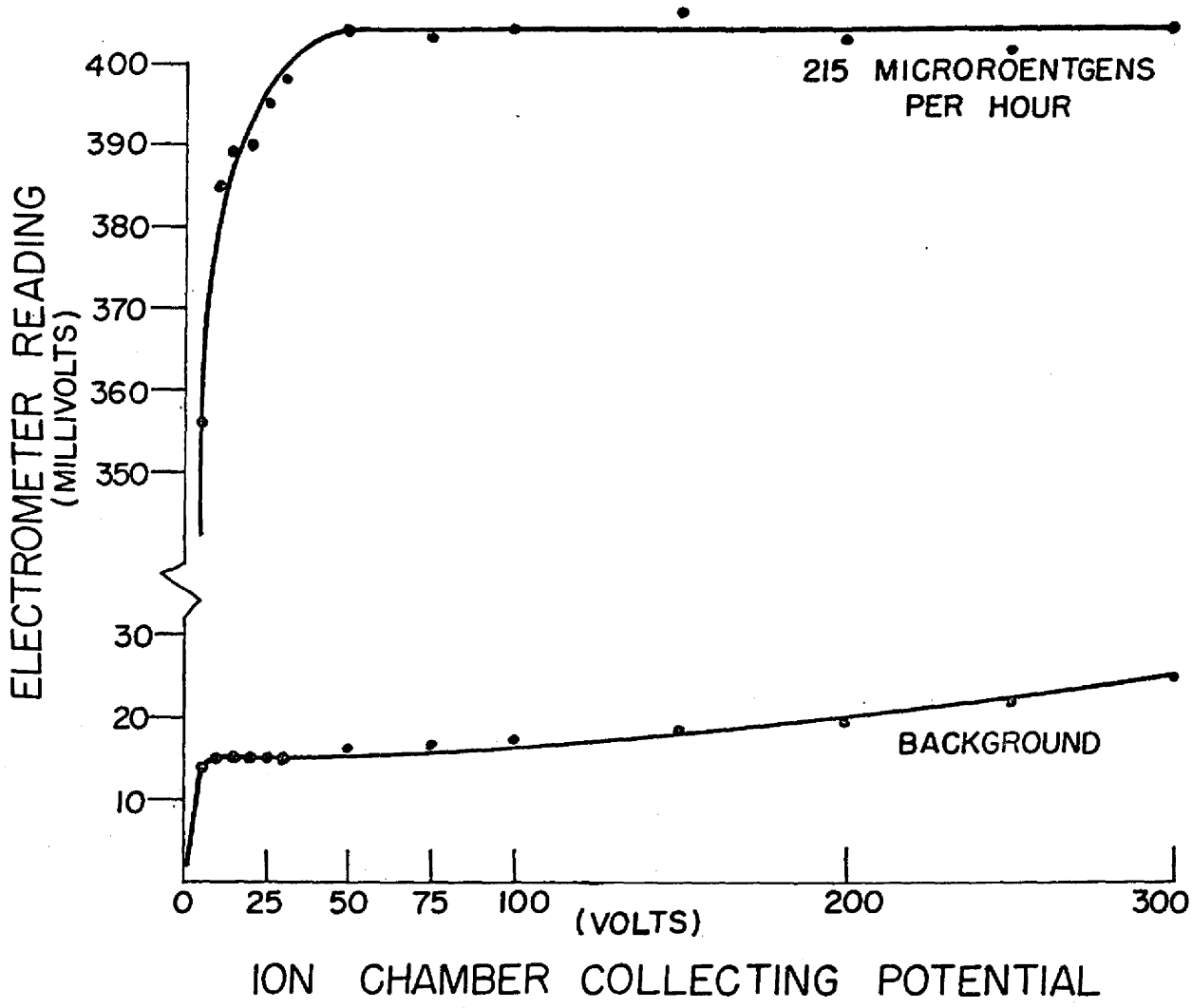
400
390
380
370
360
350
30
20
10
ELECTROMETER READING
(MILLIVOLTS)
215 MICROROENTGENS
PER HOUR
BACKGROUND
0
25
50
75
100
(VOLTS)
200
300
ION CHAMBER COLLECTING POTENTIAL

Figure II-3

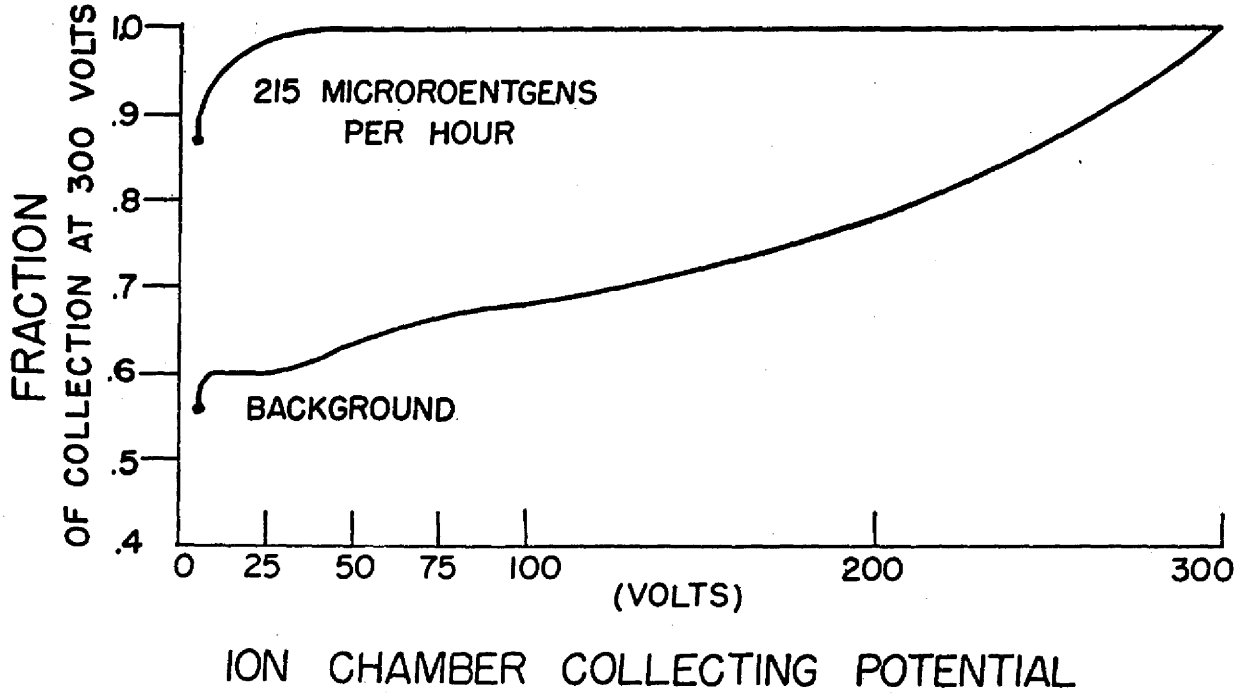
FRACTION
OF COLLECTION AT 300 VOLTS
1.0
.9
.8
.7
.6
.5
.4
215 MICROROENTGENS
PER HOUR
BACKGROUND
0
25
50
75
100
200
300
(VOLTS)
ION CHAMBER COLLECTING POTENTIAL

Figure II-4

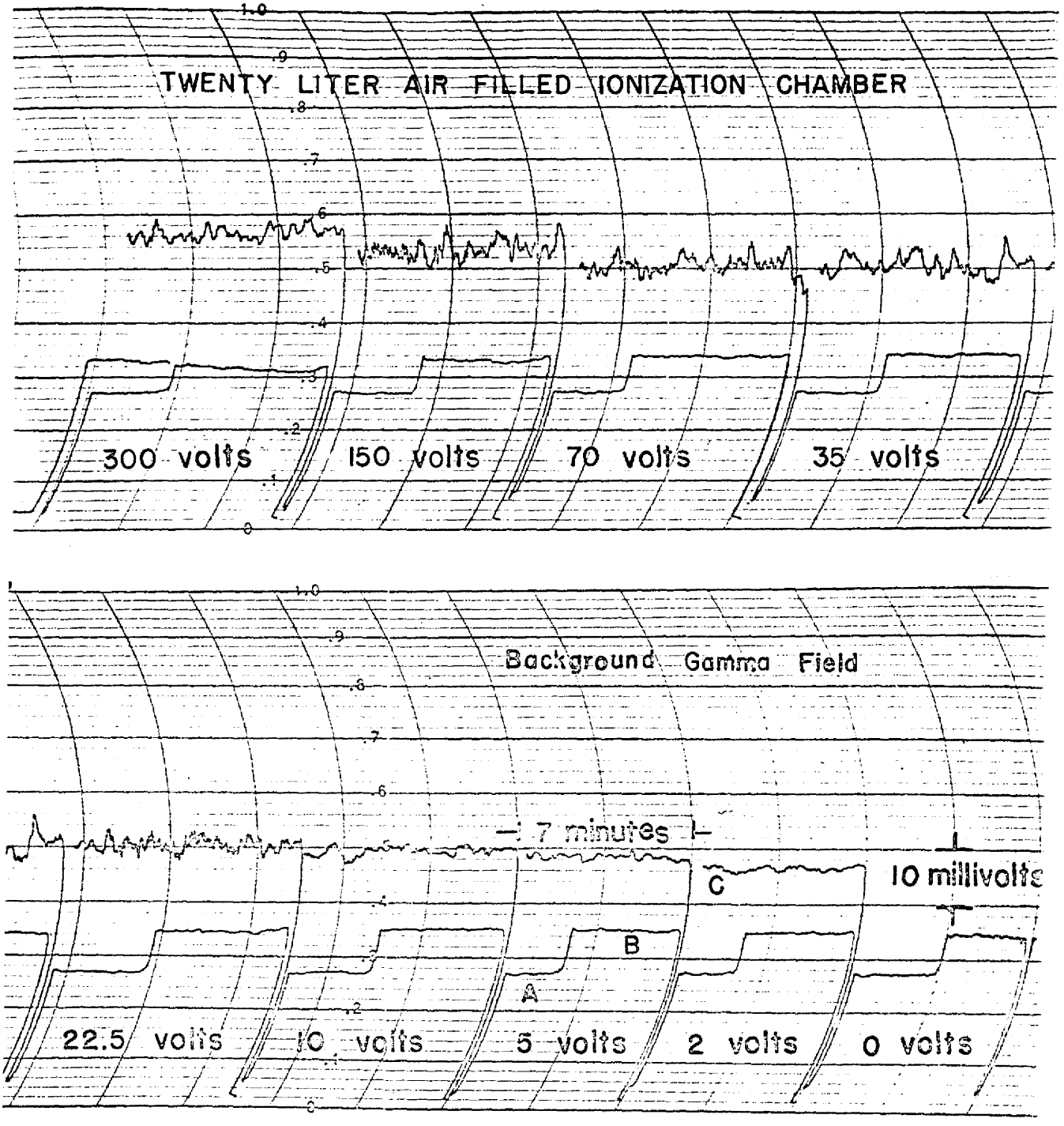

Radiation Background Traces for
Different Collecting Potentials

Figure II-5

References to Appendix II

a. Hess, V. F. and Vancour, R., Physical Review, 76, No. 8, P. 1205 (Oct. 15, 1949).

b. Wilkinson, D. H., Ionization Chambers and Counters, Cambridge, 1950, P. 51 ff.

c. Actually the 0.84 rhm figure applies to a radium needle with 0.5 mm platinum filtration. The filtration of the platinum (0.2 mm) and the aluminum holder (1.82 mm) combined is closely equivalent to a filtration of 0.43 mm platinum. In this connection, it is noted that the dose output of radium in equilibrium with its daughter products has recently been revised to 0.825 rhm/1 mg Ra with 0.5 mm platinum filtration (cf. National Bureau of Standards Technical News Bulletin, 41, 12, P. 198, Dec. 1957). Using this new figure and taking into account the slightly smaller filtration of our source, our recalculated estimate for the dose rate output would be 0.83 rhm/1 mg Ra.

d. Ohmart, P. E., et al, The Radioelectric Effect, AEC Report MLM-629 (Nov. 1, 1951).

ACKNOWLEDGMENTS

The authors are grateful for the helpful guidance of Dr. S. Allan Lough, Director of the Health and Safety Laboratory, in the preparation of this report.

They should like also to acknowledge many helpful conversations with Professor Morris H. Shamos, Chairman of the Department of Physics, New York University, on the subjects of ion chamber measurements and ion recombination in gases.

Reprinted from NUCLEAR SCIENCE AND ENGINEERING, Vol. 3, No. 1, January 1958
Academic Press Inc. *Printed in U.S.A.*

NUCLEAR SCIENCE AND ENGINEERING: **3**, 77-84 (1958)

A Semiempirical Method of Calculating the Energy Absorption Buildup Factor with an Application to a Uniformly Contaminated Space Having Spherical Boundaries

KERAN O'BRIEN, WAYNE M. LOWDER, AND LEONARD R. SOLON

Health and Safety Laboratory, New York Operations Office, U. S. Atomic Energy Commission, New York 23, New York

Received April 15, 1957

A form for the point-source gamma-ray energy absorption buildup function valid for a material in the energy range where it is essentially a Compton scatterer is suggested as a modification of the asymptotic forms derived by U. Fano. Its parameters are evaluated by means of an energy equilibrium condition and a fit to experimental data. The results are compared with those obtained by other methods, and an application to the problem of uniformly and continuously distributed point sources is discussed.

The point-source energy absorption buildup factor, as conventionally defined, is the ratio of the energy absorption rate from the total-radiation flux to that from the primary flux at some point in the material surrounding the point source. This material is assumed to be uniform and infinite in extent. The buildup function for a given source energy describes the variation of the buildup factor as a function of mean free path and will be designated by $b(t)$.

If we assume a form of the buildup function consistent with the considerations of Fano (*1*), it is possible to compute buildup factors for Compton scatterers by using an energy-equilibrium condition (*2–6*) in combination with a fit to experimental data (*7–9*).

The dose rate in a uniformly contaminated medium of infinite extent, when the contaminant is a monochromatic gamma emitter, is given by

$$I = \frac{E\mu_e}{\rho\mu_t}\int_0^{2\pi} d\phi \int_0^{\pi} d\theta \sin\theta \int_0^{\infty} \frac{dt\, b(t)e^{-t}}{4\pi} \tag{1}$$

where I is the dose rate in Mev/sec-gram, E the energy emitted by the contaminant in Mev/sec-cm^3, μ_e the energy absorption coefficient for the medium corresponding to the source energy in cm^{-1}, μ_t is the total attenuation coefficient for

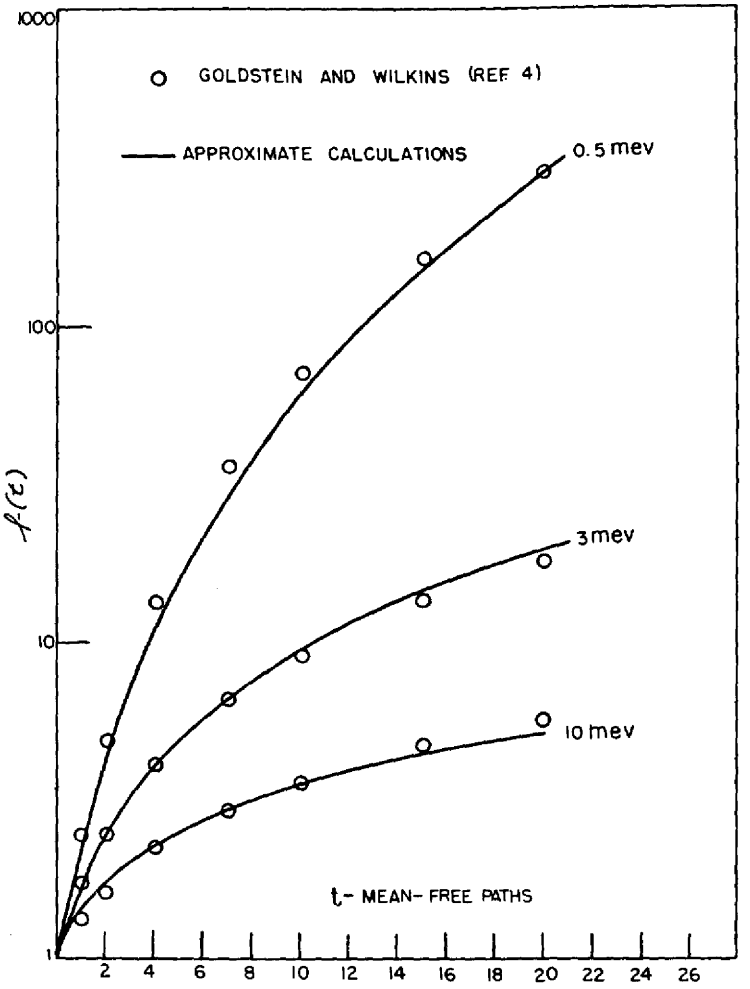

FIG. 1. Buildup factors for H_2O

the medium corresponding to the source energy in cm^{-1}, ρ is the density of the medium in g/cm^3, t the distance to a differential emitter dV in units of mean free path ($= \mu_t x$, where x is this distance in cm). The system is in spherical coordinates, and ϕ and θ are the azimuthal and altitudinal angles respectively.

According to Fano (*1*) the asymptotic form of the buildup function value of the attenuation coefficient is given by x^k. We propose to modify this and write

$$b(t) = (1 + \alpha t)^{\beta}. \tag{2}$$

If the use of a single form for the buildup function is to be justified it must be

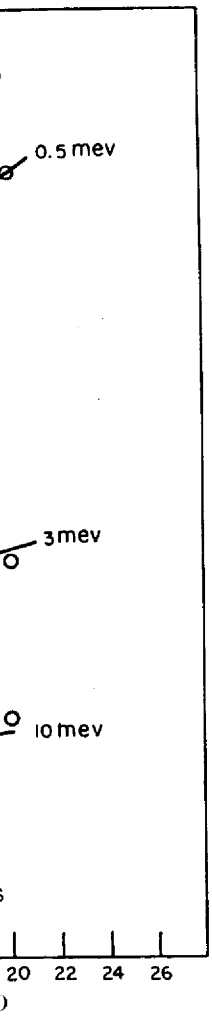

$^{-1}$, ρ is the density of the
er dV in units of mean free
stem is in spherical coordi-
angles respectively.
buildup function value of
e to modify this and write

s to be justified it must be

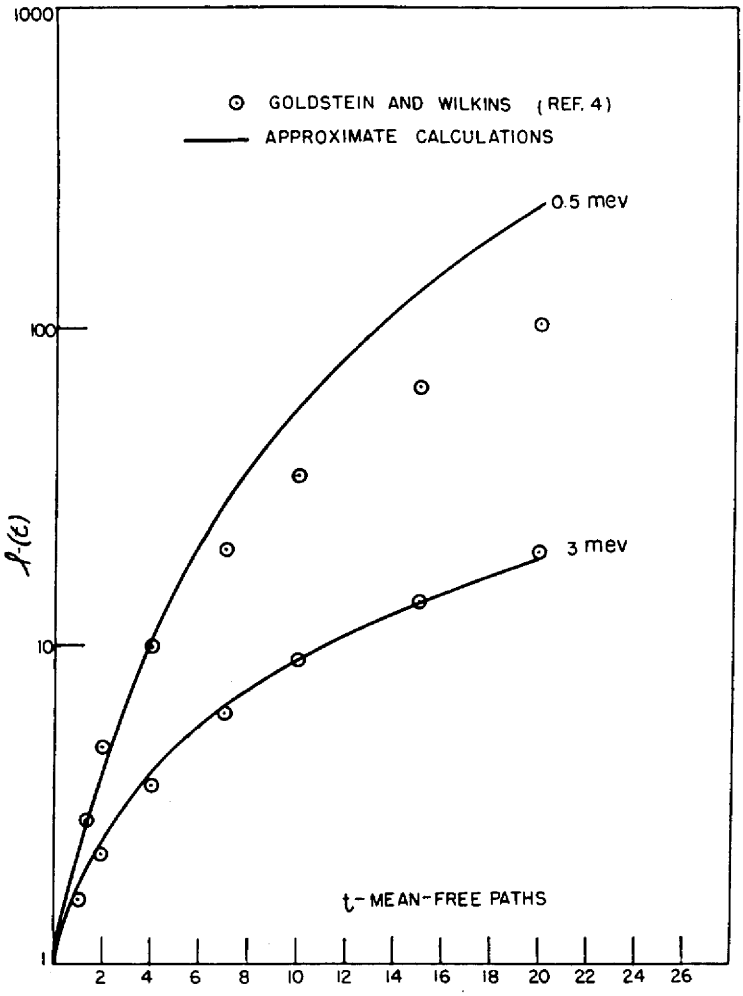

FIG. 2. Buildup factors for Fe.

confined to a region where $d\mu_t/dE_0$ (E_0 being the source energy) has a regular behavior. For this reason and because this is the region for which our experimental data are applicable, we restrict Eq. (2) to the energy region where the material is a Compton scatterer.

Substituting Eq. (2) in Eq. (1) we get an answer in terms of the incomplete gamma function:

$$I = \frac{E\mu_e}{\rho\mu_t}\int_0^\infty e^{-t}(1+\alpha t)^\beta\, dt = \frac{E\mu_e}{\rho\mu_t}\,\alpha^\beta e^{1/\alpha}\Gamma(\beta+1, 1/\alpha). \tag{3}$$

Because the rate of energy absorption per gram equals the rate of energy production (the equilibrium condition), $I = E/\rho$ and therefore

$$\int_0^\infty e^{-t}(1 + \alpha t)^\beta \, dt = \alpha^\beta e^{1/\alpha}\Gamma(\beta + 1, 1/\alpha) = y \tag{4}$$

where $y = \mu_t/\mu_c$.

Because of the way that α and β appear in Eq. (4) it is difficult to perform numerical operations using it, and for convenience we have made use of two approximations. For $y < 2.8$ we use

$$\beta = \frac{\ln [y(y - 1) + 1]}{\ln (1 + \alpha y)} \tag{5}$$

and for $y > 2.8$

$$\beta = \frac{y - 1}{\ln (1 + \alpha y)}. \tag{6}$$

These approximations are discussed in the appendix.

The buildup function now has the form

$$b(t) = \begin{cases} \exp\left\{\dfrac{\ln [y(y - 1) + 1]}{\ln(1 + \alpha y)} \ln (1 + \alpha t)\right\} & y < 2.8 \\ \exp\left\{\dfrac{y - 1}{\ln (1 + \alpha y)} \ln (1 + \alpha t)\right\} & y > 2.8 \end{cases} \tag{7}$$

Fitting Eq. (4) to the experimental data (*7–9*) we find that $\alpha \simeq 1/y$.[1] Substituting this in Eq. (7) we have for the buildup function

$$b(t) = \begin{cases} \exp\left\{\dfrac{\ln [y(y - 1) + 1]}{\ln 2} \ln \left(1 + \dfrac{t}{y}\right)\right\} & y < 2.8 \\ \exp\left\{\dfrac{y - 1}{\ln 2} \ln \left(1 + \dfrac{t}{y}\right)\right\} & y > 2.8 \end{cases} \tag{8}$$

Figures 1, 2, and 3 show comparison of Eq. (8) with the calculations of Goldstein and Wilkins (*4*). The calculations for lead and for low-energy photons on iron represent cases where departures from our assumptions become important. 500-kev photons on iron have energies close to the photoelectric region, and lead is hardly a Compton scatterer even at 1 and 2 Mev. Equation (8) agrees very poorly with the calculations of Goldstein and Wilkins for 0.255 Mev and

[1] The work of M. A. Van Dilla and G. J. Hine [*Nucleonics* **10**, No. 7, 54 (1952)] furnishes different results. For a discussion of this experiment see Ref. (*4*)

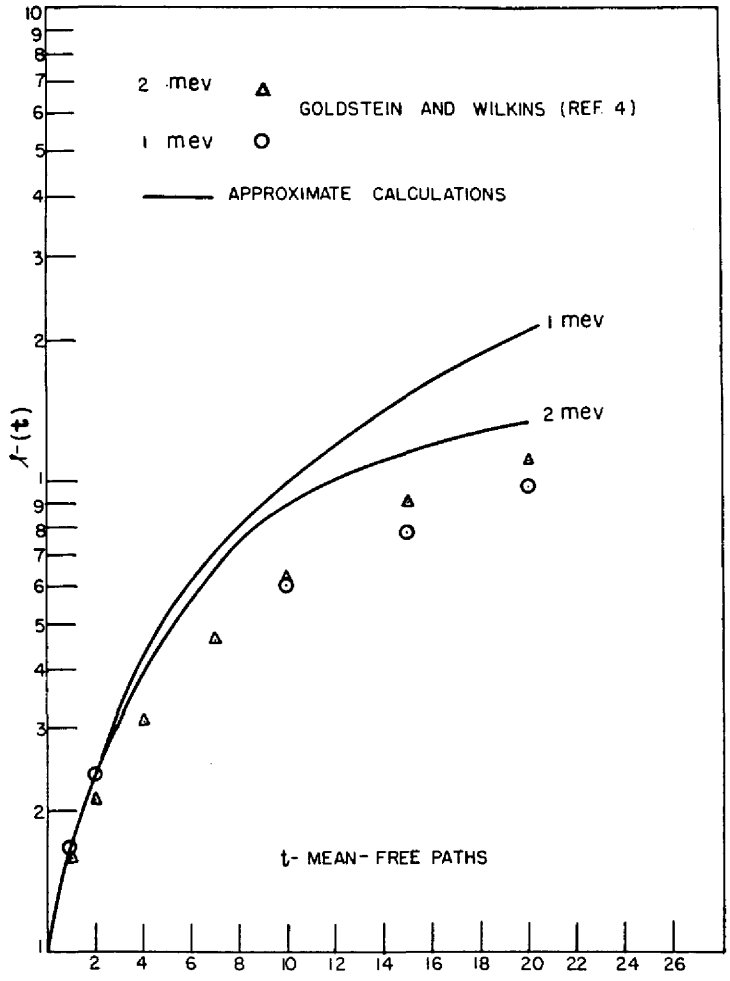

FIG. 3. Buildup factors for Pb.

water. However, experimental values for the buildup function, normalized to four mean free paths, are given for gammas from Hg^{203} (0.28 Mev) (8) and are in reasonable agreement with Eq. (8). These buildup factors are exhibited with those of Goldstein and Wilkins for comparison in Fig. 4.

It is possible to modify Eq. (1) to include the dose rate at a distance from a medium with a spherical boundary.

$$I = \frac{E\mu_r}{\mu_t \rho} \int_0^{\phi_0} d\phi \int_0^{\theta_0} d\theta \sin\theta \int_{f(\phi,\theta,t)}^{a(\phi,\theta,t)} \frac{dt(1+\alpha t)^{\beta} e^{-t}}{4\pi}. \tag{9}$$

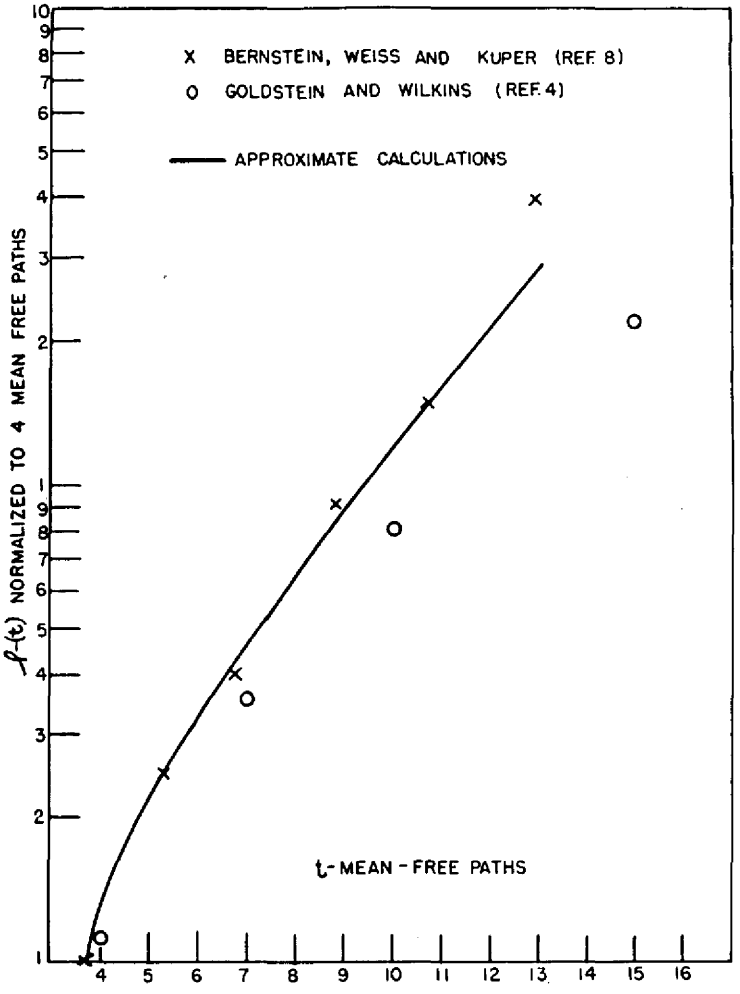

FIG. 4. Comparison of theoretical and experimental buildup factors for 0.28-Mev photons on H_2O

As this equation is rather difficult to solve exactly except for simple boundaries, we introduce another approximation. Let us expand Eq. (2) binomially, terminating it at n terms, where n is the largest integer less than $\beta + 2$. This approximation is, of course, exact when β is integral. A partial solution for Eq. (9) is then

$$I = -\frac{E\mu_e}{\rho\mu_i}\int_0^{\phi_0} d\phi \int_0^{\theta_0} \frac{d\theta \sin\theta e^{-t}}{4\pi} \sum_{\nu=0}^{n} \frac{A_\nu t^\nu}{\nu!}\Bigg|_f^a \tag{10}$$

)LON

PER (REF 8)
REF 4)

3 14 15 16

dup factors for 0.28-Mev

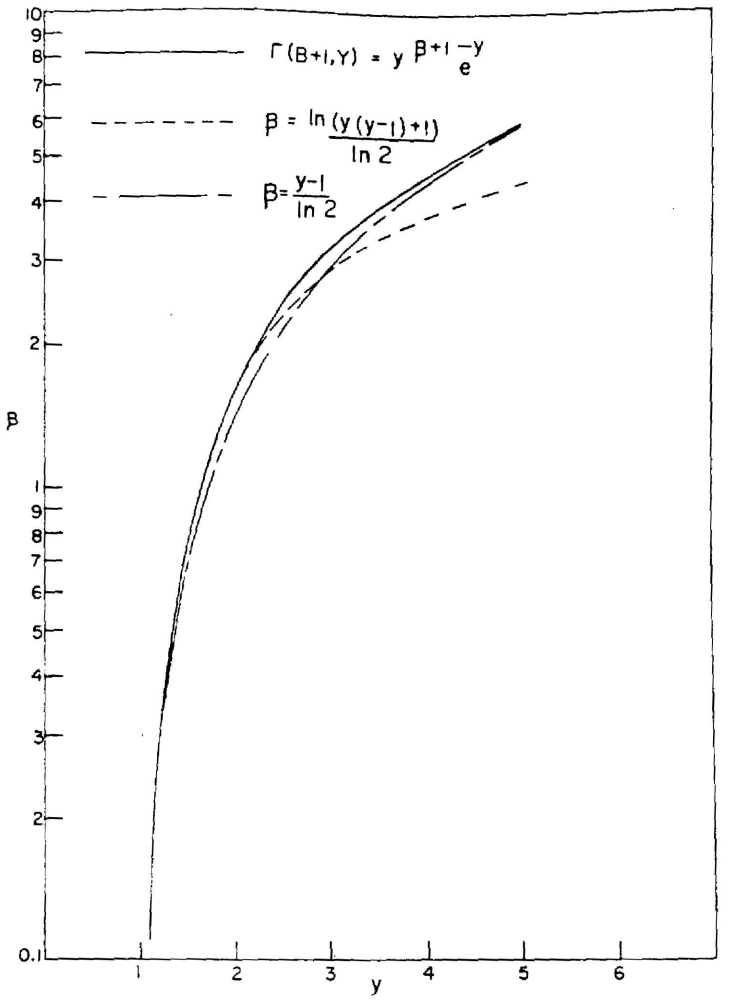

FIG. 5. Comparison of various approximations to the incomplete gamma function.

pt for simple boundaries,
(2) binomially, terminat-
$\beta + 2$. This approxima-
lution for Eq. (9) is then

$$\frac{A_\nu t^\nu}{\nu!}\Big|_0^a$$

where

$$A_0 = y$$
$$A_1 = y - 1$$
$$A_2 = y - 1 - \alpha\beta$$
$$A_3 = y - 1 - \alpha\beta - \alpha^2\beta(\beta - 1)$$
$$* \quad * \quad *$$
$$A_{n+1} = 0.$$

The case of the dose rate in air at some height t_h (mean free paths in air) over a uniformly contaminated half-space is of some interest. Here, $g = \infty$ and $f = t_h \sec\theta$, $\phi_0 = 2\pi$ and $\theta_0 = \pi/2$. The solution is

$$I = \frac{E\mu_e}{2\rho\mu_t}\left[t_h E_i(-t_h) + e^{-t_h}(B_0 + B_1 t_h + B_2 t_h^2 + \cdots)\right] \tag{11}$$

where

$$B_0 = A_0$$

$$B_i = \sum_{\nu=i}^{n-1} \frac{A_{\nu+1}}{\nu(\nu+1)}, \qquad i = 1, 2, \cdots, n-1$$

and

$$-E_i(-t) = \int_t^\infty (e^{-x}/x)\, dx.$$

APPENDIX

An integral equal to Eq. (4) and containing an exponential is

$$\int_0^\infty e^{-t/y}\, dt = y. \tag{12}$$

Clearly the integrands of Eqs. (12) and (4) intersect at some one point other than $t = 0$. A comparison of Eq. (4) and of the equations formed by setting the integrands equal indicates that this point is nearly $t = y$. If we assume it is exactly y, Eq. (6) follows immediately. For a wide range of values of α, β, and y, Eqs. (4) and (6) are very close. All parameters are positive here, of course.

It is possible to better this approximation in the region about $\beta = 1$ by noting from Eq. (4) that $\beta = 1$ implies $\alpha = y - 1$. We substitute $t_0 = y + ky/(y-1)$ and, only in the last stages letting k go to zero Eq. (5) follows.

A comparison of Eqs. (4), (5), and (6) is shown in Fig. 5 for the particular case of $\alpha = 1/y$.

REFERENCES

1. U. Fano, *J. Research Natl. Bur. Standards* **51,** 91 (1953).
2. W. F. Libby, *Science* **122,** 3158 (1955).
3. L. D. Marinelli, *Am. J. Roentgenol. Radium Therapy* **47,** 210 (1942).
4. H. Goldstein and J. E. Wilkins, Jr., NYO-3075 (1954).
5. R. D. Evans, *Am. J. Roentgenol. Radium Therapy* **58,** 754 (1947).
6. R. Loevinger, J. G. Holt, and G. J. Hine, *in* "Radiation Dosimetry", (G. J. Hine and G. L. Brownell, eds.), Chapter 17. Academic Press, New York, 1956.
7. G. R. White, *Phys. Rev.* **80,** 154 (1950).
8. W. Bernstein, M. M. Weiss, and J. B. H. Kuper, BNL-AFSWP 448(1953).
9. C. Garret and G. N. Whyte, NRC-3257 (1954).